A look into the multimodalilty future was presented by Hara et al. from Massachusetts General Hospital (Boston, MA), who reported on "Molecular imaging of deep vein thrombosis using a new fibrin-targeted near-infrared fluorescence imaging strategy" [4]. Excellent regional uptake was coregistered with the CT using this optical imaging approach (Fig. 16). The ex vivo data clearly indicated localization of the signal with the thrombus. How much this can be translated to humans, however, is in question.

Conclusion

In his Blumgart Lecture, Bengel discussed the long-term survival strategy for nuclear cardiology, which I like to cite as motivation for future researchers in our field. First, we must adapt to dynamic changes in the medical landscape, especially to link molecular imaging to therapy. The increasing specificity of therapeutic measures requires increasing specificity of diagnostic tools. Molecular imaging also provides the opportunity to create imaging-driven therapeutic strategies. We need to integrate increasing knowledge in medicine and try to identify patients who may benefit from specific targeted therapies. We must also look beyond organ borders; cell trafficking, immune signaling, inflammation, and angiogenesis occur in many disease representations and will be keys to prevention and regeneration. We finally must generate an integrative environment that maximizes imaging potential by training people in these various areas.

Marcus Schwaiger, MD
Technische Universität München
Munich, Germany

Neurosciences

The dominant topic in neuroscience this year, as last year, was β-amyloid imaging, with the number of presentations increasing to 48 from 26 in 2010. The second major area was brain tumor imaging, with 33 presentations, up from 15 last year. Dopamine transporter (DAT)/vesicular monoamine transporter (VMAT) imaging was also very topical, with the release of a clinical DAT scanning agent in the United States. Small animal imaging, especially with microPET, continues to grow, with 28 presentations this year. Nonhuman primate imaging was the topic of 18 presentations at this meeting. We have an ever-increasing variety of radioligands used in neuroscience research—57 different ligands for various neuroreceptors, transporters, pathological markers, etc., were presented at this meeting. FDG PET, however, continues to play a major role and was the topic of 69 neuroscience presentations. The major areas of research are cognitive decline/dementia, the development and application of neuroreceptor imaging ligands, brain tumor investigation, and movement disorders. Good work is also being done in psychiatric disorders, drug and alcohol abuse, epilepsy, neuroinflammation, traumatic brain injury, stroke, and the effects of chemotherapy on the brain.

β-Amyloid Pet

Chet Mathis and William Klunk at the University of Pittsburgh developed ^{11}C-PiB, the first specific amyloid PET tracer and, in collaboration with Uppsala University, Sweden, performed the first human study in 2002. We now have literally thousands of studies being carried out each year with β-amyloid imaging ligands. A presentation from the Austin Hospital (Melbourne, Australia) and a consortium of researchers from 5 other Australian centers reported on "The consequences of Aβ deposition in aging and Alzheimer's disease [AD]: results from 366 elderly patients" [121]. The participants all underwent ^{11}C-PiB PET imaging with longitudinal follow-up. The main findings included that age and genetics, as expected, have a major role in the presence of amyloid in the brain. A normal person in his or her 60s has an 11% risk of having a positive amyloid scan. This jumps to 32% in the 70s and to >50% in those older than 80 y. Within these decades the strong effect of genetics is apparent, with those individuals with the ApoE-ε4 gene allele, the most prominent gene associated with AD risk, being 3 times more likely to have a positive PiB scan than those without the gene. Serial studies in this cohort are being carried out and confirm that amyloid accumulation is a slow and gradual process, with PiB binding rising ~2%–4%/y in those with positive scans and on average by 1%/y in individuals with negative scans. Figure 17 shows a comparison of average rate of gray matter atrophy over 1 y in healthy elderly individuals with and without positive PiB scans. A greater rate of atrophy in brain areas typically most affected in AD is seen in those who have positive PiB scans. Looking at outcomes over 3 y in this study, "normal" older individuals who are PiB-positive also had about a 25% chance of converting to mild cognitive impairment (MCI) or AD, compared with a risk of only 3% in those with negative scans. Those who already had symptoms of

Christopher Rowe, MD

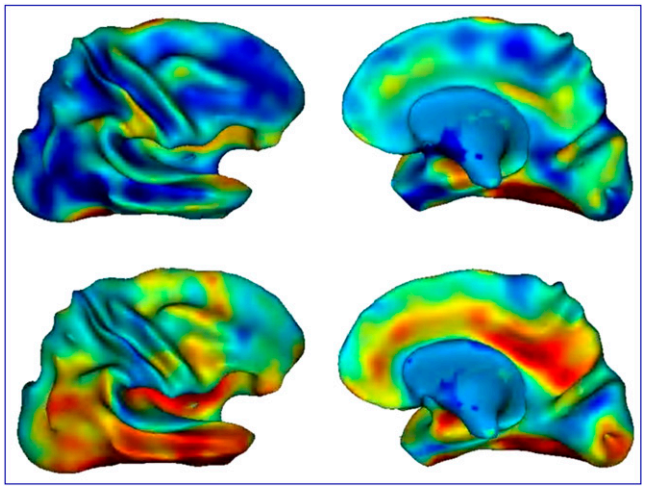

FIGURE 17. Average rate of atrophy over 1 y in healthy controls who were PiB-negative vs PiB-positive. Red areas indicate atrophic process beginning in individuals who are asymptomatic but have positive PiB scans.

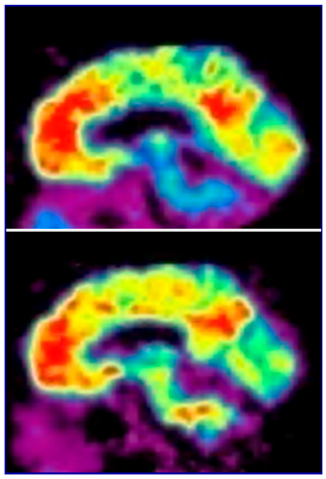

FIGURE 18. ^{11}C-PiB (top) and ^{18}F-flutemetamol (bottom) scans. For ^{18}F-flutemetamol, accuracy of visual score to correctly classify normal subjects from AD produced an area under the curve of 0.92 (95% CI 0.81–1.00).

cognitive decline but did not meet the criteria for AD and who also had a positive PiB scan had a 71% risk of developing dementia associated with AD within 3 y. It is clear that β-amyloid deposition in healthy individuals is associated with faster cognitive decline and gray matter atrophy. When PiB PET results are combined with other biomarkers of AD, such as hippocampal atrophy, the predictive accuracy in persons with MCI for developing dementia associated with AD in 3 y rises to 90%. The value of biomarkers, including imaging with FDG PET and β-amyloid PET, is now widely appreciated in the AD research and clinical communities, and these measures have recently been incorporated into recommendations for revised criteria for the diagnosis of AD and for detection of AD before dementia has developed. At this meeting 20 presentations focused on ^{11}C-PiB, compared with 12 in 2010.

The ^{18}F-labeled amyloid imaging compounds are close to clinical availability. Five abstracts were presented on ^{18}F-florbetaben (AV-1), 1 on ^{18}F-flutemetamol (3'-F'PiB), and 12 on ^{18}F-florbetapir (AV-45). Mountz et al. and researchers from the American College of Radiology Imaging Network reported on the "ACRIN-PA 4004 study: comparison of ^{18}F-flutemetamol and ^{11}C-PiB in normal control and AD subjects" [116]. Figure 18 shows excellent correlation between the 2 tracers in the same patient. Studies of the ^{18}F-florbetapir compound are now built into the extension of the Alzheimer's Disease Neuroimaging Initiative (ADNI), involving more than 800 individuals who will undergo serial ^{18}F-florbetapir studies. The introduction of ^{18}F-florbetapir to ADNI is fairly recent; before that a subgroup of 100 subjects had PiB scans. Comparison in those who have undergone both ^{18}F-florbetapir and PiB imaging shows excellent correlation (Fig. 19), although the cortical binding of PiB is greater. All 3 ^{18}F-labeled amyloid tracers reported at this meeting show greater nonspecific binding in white matter than ^{11}C-PiB, leading to less contrast between a positive and negative scan than is typically seen with ^{11}C-PiB.

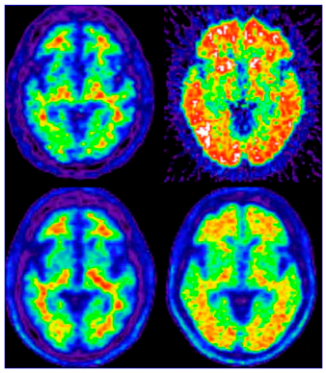

FIGURE 19. ^{18}F-florbetapir (bottom row) and ^{11}C-PiB PET (top row) scans are strongly correlated in the ADNI dataset. Left: individuals with negative scans; right: individuals with positive scans.

Sabri et al. from the University of Leipzig (Germany) and a consortium of researchers from universities in Germany and Japan reported on "Global phase 2b trial of florbetaben for β-amyloid brain PET in AD" [175]. Preliminary findings focusing on ethnic/racial differences in tracer uptake in both AD patients and healthy volunteers indicated that uptake prevalence and patterns in Japanese, Caucasians, and Hispanic/Latino individuals are similar.

Discussion has focused on optimal ways to analyze amyloid imaging studies—what should the reference region be? Joshi et al. from Avid Radiopharmaceuticals (Philadelphia, PA) reported on a method to "Determine optimal reference region to quantify florbetapir F18 brain images" [1268]. They compared using the entire cerebellum to only the pons, centrum semiovale, or cerebellum gray matter as reference region. Differences were marginal. Correlations using postmortem series data also indicated marginal differences between the various reference regions when comparing the scan binding measures to plaque density measured in postmortem brain tissue (Fig. 20). However, using the whole cerebellum as the reference region is a less exacting task than using cerebellar grey matter.

Figure 21 is a composite of examples of imaging with ^{11}C-PiB, ^{18}F-florbetaben, ^{18}F-flutemetamol, and ^{18}F-florbetapir. The color scale was set to a similar range in white matter, and areas of uptake are relatively similar in all of these scans. These are selected high-quality scans; whether they will be as easy to read when the quality is not as good or the amyloid load not as high has yet to be determined.

Interesting work was presented by Rodrique et al. from the University of Texas Southwestern Medical Center (Dallas) and the University of Texas Dallas, who reported on "β-amyloid in healthy aging: regional distribution and cognitive consequences" [119]. They looked at 137 "normal" elderly individuals with flor-

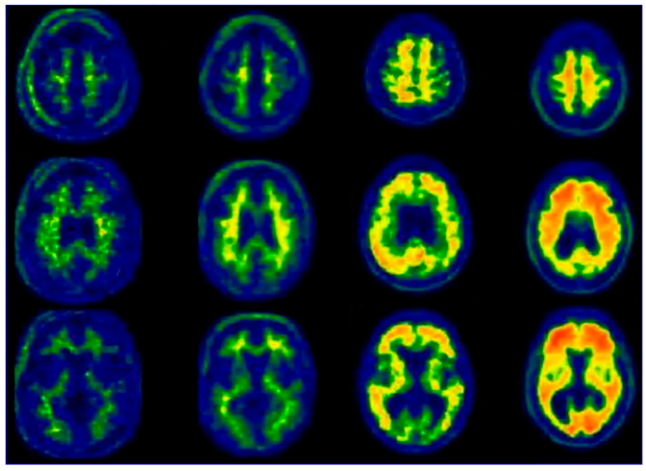

FIGURE 20. Representative ^{18}F-florbetapir PET images from A07 phase III trial. Left 2 columns: negative scans; right 2 columns: positive scans. The amount of amyloid plaque at postmortem corresponding to each scan (left to right) was low and sparse for the negative scans and moderate and frequent for the positive scans by CERAD criteria and measured 0.0%, 0.47%, 1.11%, and 9.14%, respectively, by quantitative immunohistochemistry (i.e., % of microscopic slide area occupied by plaque).

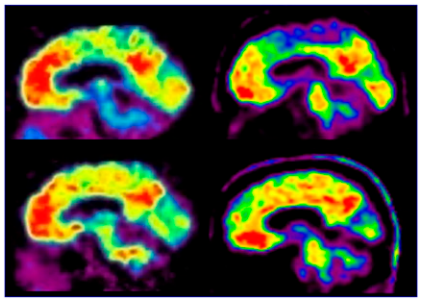

FIGURE 21. β-amyloid plaque imaging with PET and (top left) ^{11}C-PiB, (bottom left) ^{11}F-flutemetamol, (top right) ^{18}F-florbetaben, and (bottom right) ^{18}F-florbetapir.

betapir, with results again demonstrating that amyloid presence in the brain is not a good thing. In looking at the effect of mean cortical amyloid on cognition, they found a significant effect on processing speed, working memory, and fluid reasoning in those with high levels of amyloid. In a second presentation based on this same study, the group reported that "Precuneus amyloid burden correlates with cortical network dysfunction in a sample of healthy aging adults" [169]. They showed problems with functional connectivity in areas of amyloid binding (Fig. 22). In a third presentation from this group, Kennedy et al. reported that "Precuneus amyloid burden is associated with decreased bilateral frontal activation and default network suppression in healthy adults" [1269]. These studies in apparently healthy elderly persons provide further evidence that amyloid deposition as measured by ^{18}F-labeled amyloid imaging agents is associated with functional consequences and impaired brain performance. (Fig. 23).

Ong et al. from Austin Hospital, the Mental Health Research Institute, and the University of Melbourne (all in Melbourne, Australia), and Bayer Schering Pharma (Berlin, Germany) reported on "Conversion from MCI to AD over 12 months: predictive value of Aβ imaging with ^{18}F-florbetaben" [170]. Forty patients with MCI have been followed for 18 to 24 mo. About 50% were florbetaben-positive. Seventeen have developed AD, and 4 have developed other dementias. Using either an SUV cutoff or visual analysis, the accuracy of a positive scan in predicting those who would convert to AD was high and similar to the reported predictive accuracy of PiB PET. Figure 24 is an example of 2 elderly patients with MCI, one of whom had a negative florbetaben scan and remained stable, whereas the other, with a positive scan, progressed to AD within 2 y.

The interpretation of these scans can be challenging because of the high nonspecific white matter uptake that may exceed cortical binding in positive individuals. Figure 25 shows examples of negative and positive florbetapir scans. One of the predominant differences is the loss in the positive study of the distinct white matter pattern seen in the negative study. The interpretation of these scans may rely somewhat on this loss of white matter pattern, with activity extending out to the edge of the cortex as a good way to pick up the presence of cortical amyloid.

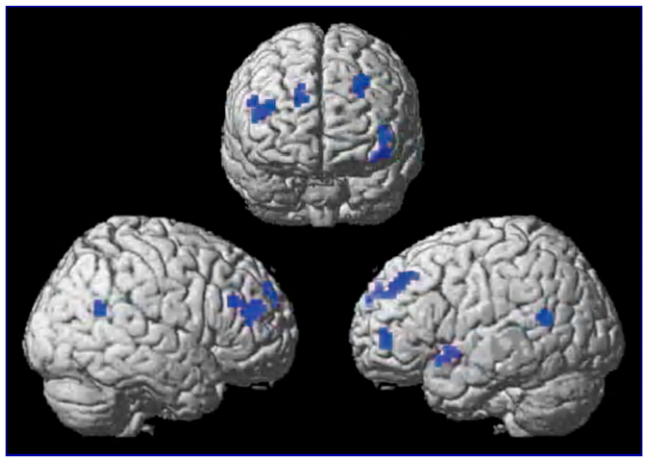

FIGURE 23. Greater precuneus β-amyloid is associated with decreased prefrontal activation in passive encoding (areas in blue). Participants viewed images and later recalled these images in the scanner. Results indicated a dose–response relationship between amyloid burden and neural activation strength.

To assist in the interpretation process, programs are being developed to automatically assess scans. Zubal et al. from Molecular NeuroImaging, LLC (New Haven, CT), Bayer Healthcare Pharmaceuticals (Berlin, Germany), and the University of Leipzig (Germany) reported on "An automated, operator-independent method for quantitative analysis of florbetaben PET scans to assist in the differential diagnosis of dementia" [2054]. Barthel et al. from the University of Leipzig (Germany), Hermes Medical Solutions (Stockholm, Sweden), IBRI (Kobe, Japan), Molecular

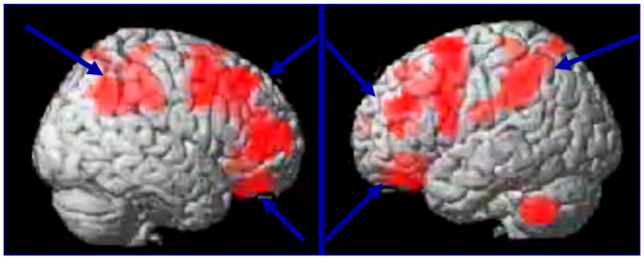

FIGURE 22. Regions where increasing β-amyloid burden decreases connectivity. Arrows point to lateral parietal, dorsolateral prefrontal cortex, and orbitofrontal cortex areas.

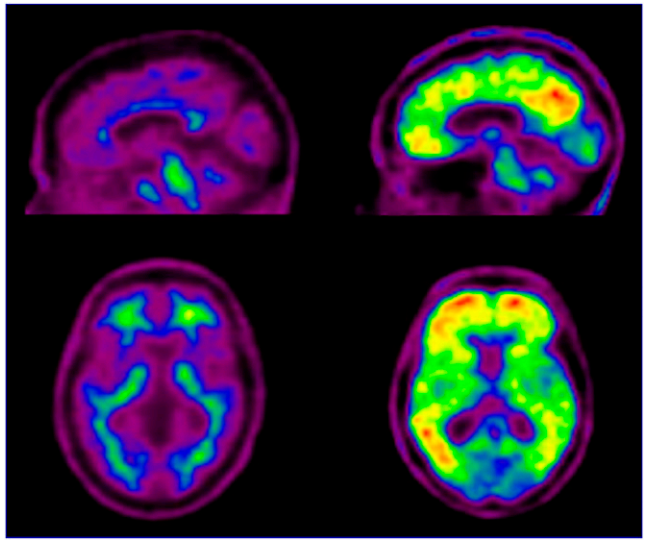

FIGURE 24. ^{18}F-florbetaben PET images in 2 patients with MCI, both of the same age and MMSE score of 26. Subject on left remained stable, whereas subject on right developed AD within 2 y.

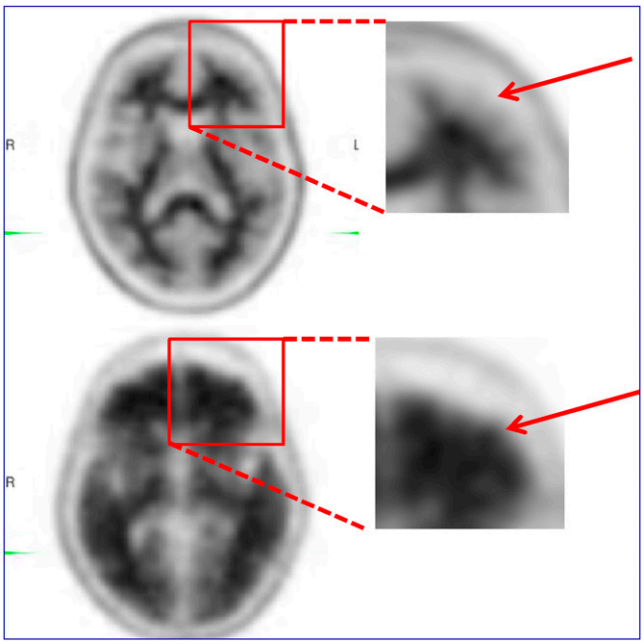

FIGURE 25. Examples of negative and positive florbetapir scans that illustrate the loss of white matter pattern when amyloid is present.

NeuroImaging, LLC (New Haven, CT), and Bayer Healthcare (Berlin, Germany) reported on "Florbetaben PET and the Hermes BRASS tool for automated regional and voxelwise quantification of β-amyloid brain load" [1254]. Both studies described encouraging results.

Zha et al. from the University of Pennsylvania and Avid Radiopharmaceuticals, Inc. (both in Philadelphia, PA), reported on "^{18}F-AV-45 dimer: a PET agent for mapping vascular β-amyloid deposits in cerebral angiopathy" [27]. The amyloid in plaques in the extracerebral space is also found in vessels, where it leads to micro- and macrohemorrhages in the brain by weakening the vessel wall. The goal was to put 2 AV-45 molecules together to reduce the ability to cross the normal blood–brain barrier while retaining binding affinity to β-amyloid aggregates. The results suggest that this is a viable approach to developing an agent that can distinguish amyloid angiopathy from amyloid plaques (Fig. 26).

The ADNI, funded by the U.S. National Institutes of Health and a consortium of industry partners, has been running for more than 3 y, with >58 sites in the United States and Canada and >800 participants. Although ADNI was initially driven by MR imaging specialists, 50% of those imaged also underwent ^{18}F-FDG PET. Toward the end of the study it became quite apparent that amyloid imaging had much to add. PiB imaging was added for 100 subjects, but in the first 3-y extension to the ADNI project, which commenced this year, amyloid imaging is being performed in 100% of participants.

ADNI data are available for analysis; anyone can go to the Web site and get the images and analyze them in any way he or she chooses. This was done by Herholz et al. from the University of Manchester (UK), who reported on "Assessment of progression in MCI and AD by a calibrated FDG PET score" [1262]. They looked at the subject sample size required for a therapeutic trial to achieve a 25% benefit. They found that with FDG far fewer subjects are needed to demonstrate benefit than when using cognitive measures. They also showed that in MCI subjects who progressed to AD, the degree of hypometabolism as assessed by FDG PET was significantly worse than in those individuals who remained stable.

Mason et al. from the University of California at Los Angeles (UCLA) reported on "Value of FDG PET in predicting dementia within 3 years among patients clinically diagnosed with MCI" [1249]. This group took ADNI data on 114 individuals with MCI (76 nonprogressive and 38 progressive) and developed a dementia prognosis index looking at metabolism in areas typically affected by AD. Results showed that those who progressed had markedly reduced metabolism compared with those who did not. Conversely, they concluded that if metabolism in posterior brain areas was 4% or more above average whole brain (gray matter) activity, there was a >93% probability of remaining cognitively stable for at least 3 y (Fig. 27). In addition to predicting conversion to dementia, the magnitude of metabolic deficit indicated by this dementia prognosis index is predictive of the rate of cognitive deterioration as measured by decline in Mini-Mental State Examination (MMSE) score.

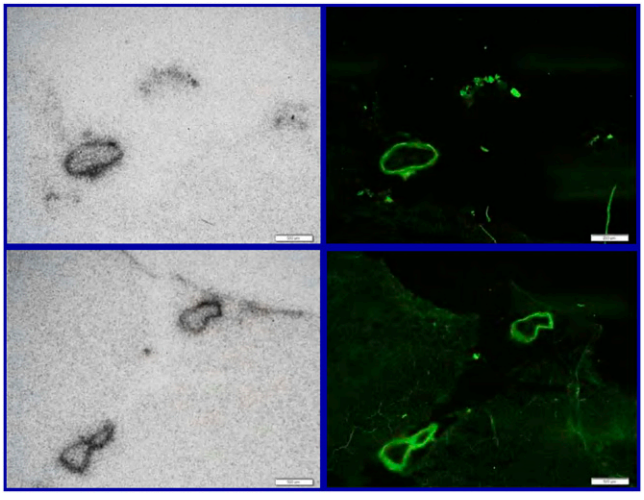

FIGURE 26. Autoradiography (left) and fluorescent imaging (right) of ^{18}F-8a (top row) vs thioflavin S staining (bottom row).

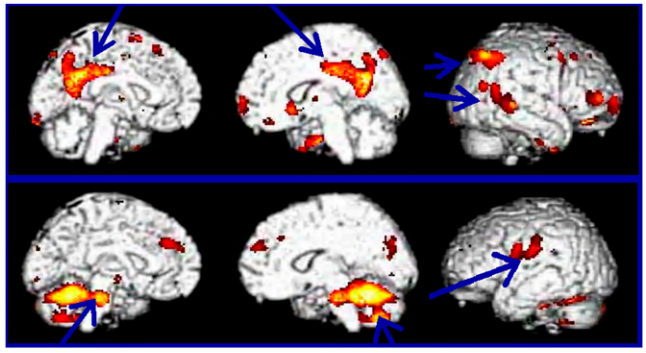

FIGURE 27. Predictive value of dementia prognosis index. Top: less metabolically active regions among progressive MCI subjects included posterior cingulate cortex and parietal temporal cortex. Bottom: relatively metabolically preserved regions among progressive MCI subjects included pons/midbrain, cerebellum, and sensorimotor cortex.

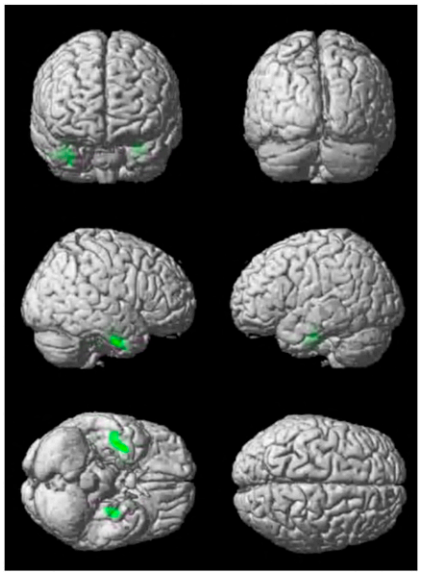

FIGURE 28. Group comparison, baseline versus follow-up, demonstrating the mesial temporal areas where treatment reduced decline in glucose metabolism that was seen in the placebo group.

Future Diagnosis And Treatment of AD

In the not-too-distant future effective treatments for AD may be available, and with effective treatment will come increasing demand for brain FDG and β-amyloid PET. Persons at risk for AD, including those with subjective memory complaints, ApoE-ε4 carriers, those with a family history of AD, or individuals showing decline on cognitive testing, will require further investigation such as β-amyloid imaging or cerebrospinal fluid (CSF) testing. If positive, treatment to reduce β-amyloid burden could be initiated well before dementia has developed. How close is that future? A few studies have reported the effect on cerebral metabolism assessed with FDG PET of antibody therapies for AD. Rominger et al. from the University of Munich (Germany), Philipps University (Marburg, Germany), Octapharma Pharmazeutika (Vienna, Austria), and Rheinische Friedrich-Wilhelms-University (Bonn, Germany) reported on the "Effect of 6 months intravenous immunoglobulin treatment on brain glucose metabolism in patients with mild to moderate AD: a phase II double blind, placebo-controlled multicenter study" [64]. The study included 44 patients with mild-to-moderate AD who were assessed by ^{18}F-FDG PET at baseline and 6 mo after initiation of intravenous immunoglobulin treatment or after placebo. They found less decline in glucose metabolism in the medial temporal regions in those under treatment than in those on placebo (Fig. 28). This is creating quite a bit of interest. Unfortunately, immunoglobulin is not easy to come by, but it is fairly nontoxic and could become a valuable tool. Before administration, however, it will be essential to know whether the patient has AD, a question that can be answered by amyloid scanning.

Other neurodegenerative diseases also lend themselves to imaging. Ma et al. from the North Shore–Long Island Jewish

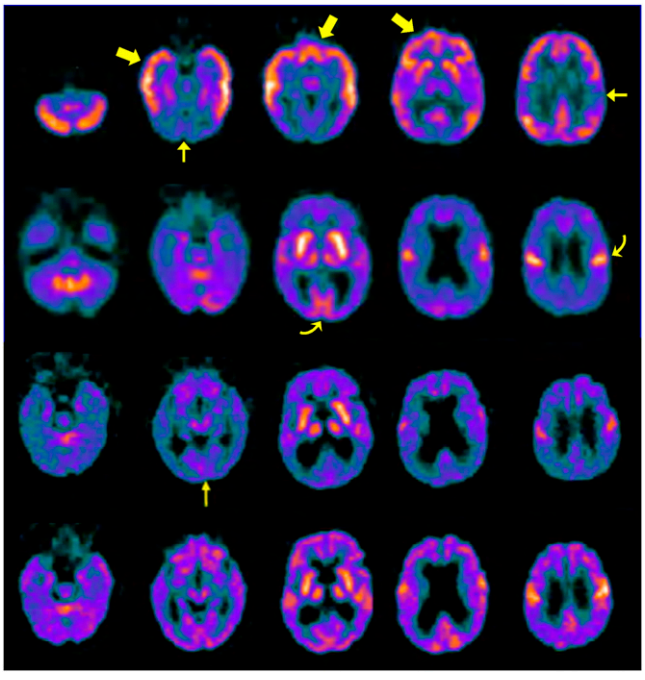

FIGURE 29. Two distinct ^{18}F-FDG PET scan patterns in NPALE. Top row: pattern 1, mixed hyper/hypometabolic. Next row: pattern 2, "neurodegenerative"—in these patients hypometabolism was seen diffusely in cortex, with sparing of primary visual cortex and sensorimotor strips (arrows), mimicking AD. Two bottom rows: Another case of "neurodegenerative" before (third row) and after (bottom row) treatment with corticosteroids demonstrated marked improvement.

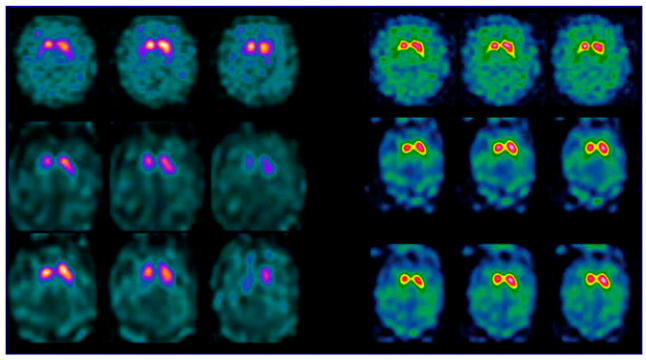

FIGURE 30. DaTscan SPECT images in a patient with tremor in the left upper limb. The top row shows images acquired over 35 min with a dual-head γ camera. Middle and lower row are images acquired for 10 and 5 min, respectively, with a CZT camera. Images are displayed in 2 color scales.

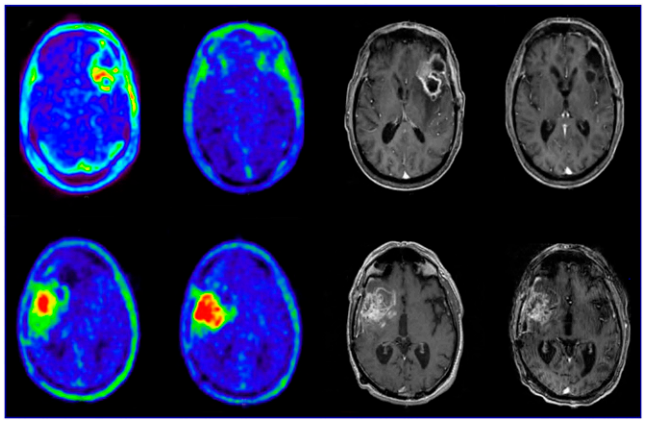

FIGURE 31. ^{18}F-FLT PET images of glioblastoma patients (top row, responder; bottom row: nonresponder) on bevacizumab therapy imaged at baseline and 6 wk (left image set) and MR at baseline and 6 wk (right image set).

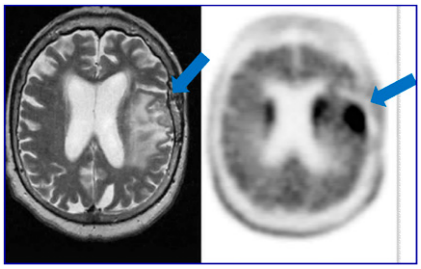

FIGURE 32. Level of suspicion in this patient with a grade III astrocytoma went from moderate on T2-weighted MR imaging (left) to high with ^{18}F-FDOPA PET (right).

Health System (Manhasset, NY) reported on "Reduced dopamine D_2 receptor binding in striatal subregions in presymptomatic Huntington's disease [HD]: a longitudinal ^{11}C-raclopride PET study over 7 years" [555]. The researchers found a steady loss of striatal D2 receptor in presymptomatic HD gene carriers before and after reaching early clinical phases of the disease and that D_2 receptor imaging can predict time to clinical onset in presymptomatic HD gene carriers.

Patel et al. from Baylor College of Medicine and the Methodist Hospital (both in Houston, TX) reported on "^{18}F-FDG PET in a reversible form of dementia: unexpected patterns of brain glucose metabolism in nonparaneoplastic autoimmune limbic encephalitis [NPALE]" [1238]. NPALE is a rare but treatable condition. Patients present with dementia, psychotic/affective symptoms, behavioral abnormalities, and sometimes seizures. It is underdiagnosed and potentially fatal if untreated. Patients usually respond to intravenous corticosteroids. The study included 9 patients, in whom the researchers identified 2 patterns they termed mixed hyper/hypometabolic and "neurodegenerative" (Fig. 29). The second could be easily mistaken for advanced neurodegenerative disease. Figure 29 also shows a case that improved remarkably on corticosteroid medication. The authors concluded that FDG PET neuroimaging can help in diagnosing NPALE and that it is important to be aware of the 2 striking and different metabolic patterns.

DAT/VMAT Imaging

Programs are being developed to automate the analysis of DAT and VMAT images, with goals to develop robust methods and to implement a standard cut-off score for normality that will be applicable across institutions. Zubal et al. from the Institute for

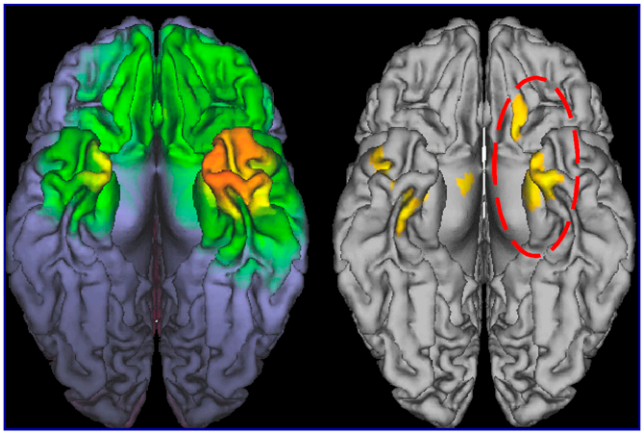

FIGURE 33. Imaging with cell phones on vs off showed significant increases in glucose metabolism in right orbitofrontal cortex and lower right temporal gyrus. Left: estimated radiofrequency amplitudes to the brain. Right: areas of increased glucose metabolism with cell phone activation.

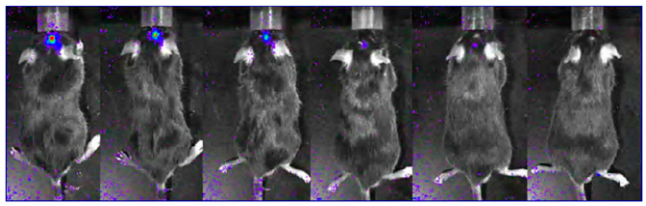

FIGURE 34. In vivo bioluminescence imaging at d 2–10 (L to R) after NSC-FLUC cell transplantation in mouse model of Parkinson disease.

Neurodegenerative Diseases (New Haven, CT) and the Sourasky Medical Center (Tel Aviv, Israel) reported good results in "Automated program for analyzing striatal uptake of DaTscan SPECT images in humans suspected of Parkinson's disease" [2098].

Baillez et al. from the Polyclinique du Bois, the Hopital St. Philibert, and the Groupe Hospitalier de l'Institut Catholique de Lille (all in Lille, France) reported on "DaTscan SPECT on a new CZT camera: from phantom to preliminary clinical validation" [2013]. Preliminary clinical studies indicate that morphology and asymmetry are relatively consistent with standard γ camera acquisition, but much shorter acquisition times are possible. Positioning, however, is crucial and not all patients can sit in the required position for 10 min. As seen in Figure 30, the rest of the brain is quite nonuniform, indicating that further studies are needed.

Brain Tumor Imaging

Many tracers for brain tumor imaging were described in presentations at this meeting, among them ^{18}F-FDG (9 presentations), ^{11}C-methionine (5), ^{11}C-acetate (1), ^{11}C-choline (1), ^{18}F-FET (6), ^{18}F-FLT (5), ^{18}F-fluorodopa (4), and ^{18}F-FMISO (1). Schwarzenberg et al. from UCLA, for example, reported on "^{18}F-FLT PET uptake dynamics and overall survival predictions for patients with recurrent high-grade glioma on bevacizumab therapy" [274]. Figure 31 shows 2 patients with recurrent glioblastoma, 1 a responder and 1 a nonresponder to bevacizumab therapy. Median time to death for responders in this study was 12.5 mo and for nonresponders only 3.8 mo.

Walter et al. from UCLA reported on the "Impact of ^{18}F-DOPA PET/CT imaging on the management of patients with brain tumors: the referring physician's perspective" [275]. They administered questionnaires to the managing physician before and after imaging in 58 patients and found significant effects on manage-

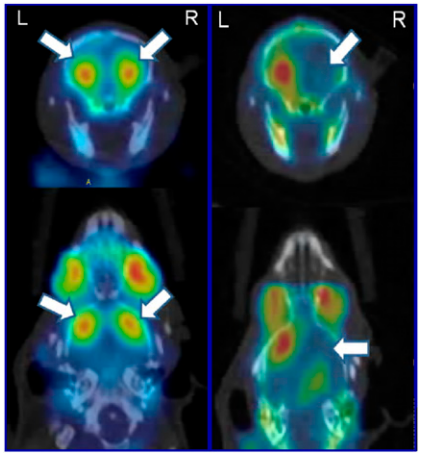

FIGURE 35. Significantly reduced DAT in Parkinson disease mice was not reversed after neural stem cell transplantation. Left: control mouse; right: Parkinson disease mouse.

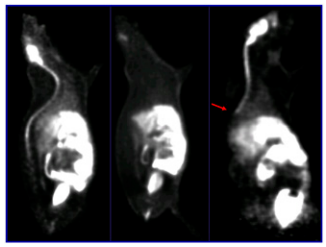

FIGURE 36. ^{11}C-AFM images. Left to right: control scan in a healthy rat; blocking scan in a healthy rat after 2 mg/kg citalopram, spinal cord injury (SCI) rat (arrow, lesion site).

ment. Management changes were planned in 24 (41%) patients as a result of scanning. Figure 32 shows a grade III anaplastic astrocytoma for which the level of suspicion was changed by imaging from moderate to high and management was changed from watchful waiting to chemotherapy.

Management impact studies are essential to transitioning new scans into clinical practice, but we need to go further and pursue comparative effectiveness research. We need to know, for example, the actual cost of investigations and whether a management change actually benefits the patient. Without this and other information, it will be extremely difficult to get insurers and other payers to meet the cost of new scans.

Other Applications

Volkow et al. from the National Institute on Drug Abuse (Bethesda, MD) and Brookhaven National Laboratory (Upton, NY) reported on the "Effects of cell phone radiofrequency signal exposure on brain glucose metabolism" [60]. They found that cell phones cause a regional increase in brain metabolism. Forty-seven participants underwent 2 ^{18}F-FDG PET scans, 1 d with a cell phone on and another with it off. For both scans, 2 cell phones, 1 on the left and 1 on the right ear, were used to avoid confounding effects from expectation. Figure 33 shows the calculated effect of radiofrequency amplitude and the metabolic effect. They also found that the closer the antenna, the larger the increase in metabolism.

Im et al. from Seoul National University College of Medicine (Korea) reported on "In vivo visualization of neural stem cells [NSCs] expressing high sensitive optical imaging reporters in mouse model of Parkinson's disease" [7]. The researchers were able to successfully monitor transplanted firefly luciferase–loaded stem cells with their in vivo bioluminescence imaging system (Fig. 34). The mice responded with functional recovery, but significantly reduced DAT density in the striatum imaged with PET was not reversed after NSC transplantation (Fig. 35).

Another interesting animal study with a number of potential human applications came from Huang et al. from Yale University School of Medicine (New Haven, CT), who reported on "Monitoring spinal cord injury and treatment outcome with PET imaging" [62]. They looked at ^{11}C-AFM PET imaging of the serotonin transporter in the rat spinal cord. They induced injury by midthoracic transection and imaged the rats at 6–12 wk after injury, calculating the lumbar/cervical ratio. Imaging showed that serotonin transporter binding went all the way down the spinal cord to the site of injury and then was lost (Fig. 36). Various forms of therapy were assessed, including immunoglobulin and the "Nogo"

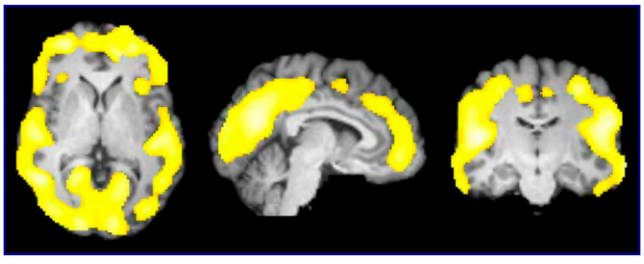

FIGURE 37. CB_1 receptors are region-specifically downregulated in cannabis smokers.

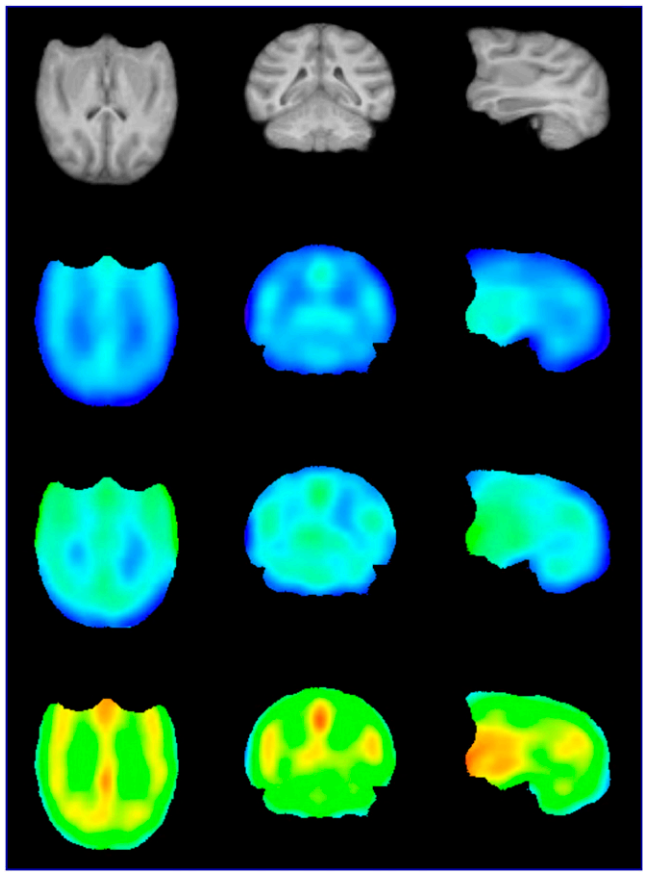

FIGURE 38. Top row: MR images; next 3 rows: ^{11}C-PBR28 images at baseline and at 1 and 4 h.

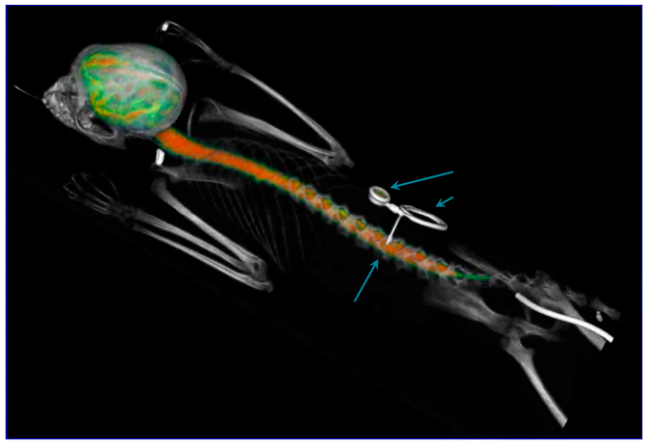

FIGURE 39. Whole-body microPET/CT image 1 h after lumbar intrathecal injection of ^{124}I-labeled arylsulfatase A. Protein is distributed over the entire leptomeningeal compartment. Top arrows: injection port and catheter. Bottom arrow: injection site.

CMIIT Sponsors Cardiovascular Symposium at NIH

The centerpiece of SNM Center for Molecular Imaging Innovation and Translation (CMIIT; formerly the Molecular Imaging Center of Excellence) activities each year is an annual multimodality molecular imaging symposium at the National Institutes of Health (NIH). In 2012, CMIIT will sponsor the "Multimodality Cardiovascular Molecular Imaging Symposium," to be held April 19–21 at the Natcher Auditorium on the NIH campus in Bethesda, MD. The proceedings of the last cardiovascular symposium in 2009, led by the CMIIT in conjunction with several other cardiovascular imaging societies, were published as a supplement to *The Journal of Nuclear Medicine* (http://jnm.snmjournals.org/content/vol51/Supplement_1/index.dtl).

The CMIIT program committee has designed a 2.5-d symposium to bring together individuals from multiple scientific disciplines, including chemistry, engineering, physics, molecular biology, cardiovascular physiology, and imaging scientists, with the goal of promoting cardiovascular molecular imaging. The speaker roster includes experts in new imaging probes and technology, imaging of cardiovascular receptors, stem cell therapy, vascular biology, myocardial metabolism, and other biological processes relevant to the cardiovascular system. The symposium will emphasize interaction among speakers and registrants to stimulate further growth in the field.

Albert J. Sinusas, MD

Sessions will review the current state of imaging in cardiovascular disease, from novel probes for evaluation and treatment of cardiovascular disease to evaluation of stem cell therapy. Challenges to translation of molecular imaging and therapy also will be addressed. These lectures will provide an overview of the potential of molecular imaging for improving understanding and management of critical cardiovascular pathophysiological processes, such as atherosclerosis, angiogenesis, cardiomyopathies, ischemia, and infarction.

The call for abstracts opens on November 14, 2011. Those abstracts accepted for presentation will be published in *The Journal of Nuclear Medicine*. Travel awards will be available to young investigators. For additional information, visit www.snm.org/cvmi2012.

Albert J. Sinusas, MD
Chair, Cardiovascular Molecular Imaging
Symposium Program Committee

receptor decoy protein, and reimaged over the course of 3 mo. They saw an increase in serotonin transporter binding associated with improved therapeutic results.

Hirvonen et al. from the University of Turku (Finland), the National Institute of Mental Health (Bethesda, MD), and the National Institute on Drug Abuse (Baltimore, MD) reported on "Reversible and regionally selective down-regulation of brain cannabinoid CB_1 receptors in chronic daily cannabis smokers" [10]. Being a daily cannabis smoker was shown to have measurable effects throughout the brain (Fig. 37), with CB_1 receptors region-specifically downregulated. This downregulation also correlated with years of abuse. However, CB_1 receptors were found to increase after abstinence.

Neuroinflammation ligands have been an area of both great promise and disappointment. Studies with ^{11}C-PK11195, the first ligand for the peripheral benzodiazepine receptor that is expressed on activated inflammatory response cells, have been hindered by high nonspecific white matter uptake and poor image quality. This receptor is now referred to as the transporter protein (TSPO). Recently developed TSPO ligands have better imaging characteristics but have revealed that marked heterogeneity exists in the degree of binding in normal persons. Hannestad et al. from Yale University School of Medicine (New Haven, CT) reported on "Experimental endotoxemia and microglial activation: a PET study in nonhuman primates" [499]. Their aim was to measure whether binding of a new TSPO ligand, ^{11}C-PBR28, increases after systemic endotoxin administration in baboons. The baboons underwent PET imaging at baseline and 1, 4, and 24 h after endotoxin infusion. Figure 38 shows that an acute reaction was readily detected by PET imaging. Much work continues in this field because of the many potential applications for imaging neuroinflammation.

Finally, another animal study posed the question of whether there is a back door to the brain for biomolecules. Belov et al. from Massachusetts General Hospital, Harvard Medical School, and Shriners Hospitals for Children (all in Boston, MA) looked at "Iodine-124 for quantitative PET imaging of macromolecule transport to CSF" [1195]. Tracer was administered into the lumbar space in nonhuman primates (Fig. 39). The brain was imaged over various time periods (0.5, 2.5, 5, and 24 h), and the initial CSF distribution of the tracer was subtracted from later images. Results show that the tracer made it into the brain tissue. This group concluded that intrathecal administration of enzyme replacement therapeutics may be beneficial for the therapy of the central nervous system component of lysosomal storage diseases.

Conclusion

Molecular imaging continues to have an important role in drug development and basic discovery in neuroscience. Clinical applications in neurodegenerative disease are set to expand substantially with better use of FDG, wide availability of ^{18}F-labeled β-amyloid ligands, and a DAT SPECT ligand now available in the United States and many other parts of the world. Clinical demand will rise greatly once an effective treatment for AD is found. We are likely to see an evolving role for PET imaging in brain tumor management. The future is bright, but clinical acceptance will depend on comparative effectiveness research, which has yet to be fully embraced by the molecular imaging community.

Christopher Rowe, MD
Austin Health
Melbourne, Australia